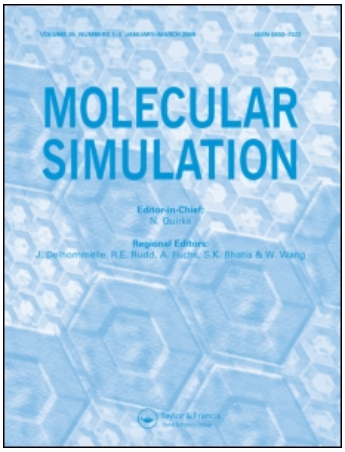

Molecular Simulation
Publication details, including instructions for authors and subscription information:
http://www.informaworld.com/smpp/title~content=t713644482

Molecular modelling study on human histamine H1 receptor and its applications in virtual lead identification for designing novel inverse agonists

Sundarapandian Thangapandian[a]; Shalini John[a]; Sugunadevi Sakkiah[a]; Keun Woo Lee[a]
[a] Department of Biochemistry and Division of Applied Life Science (BK21 Programme), Environmental Biotechnology National Core Research Center (EB-NCRC), Gyeongsang National University (GNU), Jinju, Republic of Korea

Online publication date: 10 February 2011

To cite this Article Thangapandian, Sundarapandian , John, Shalini , Sakkiah, Sugunadevi and Lee, Keun Woo(2011) 'Molecular modelling study on human histamine H1 receptor and its applications in virtual lead identification for designing novel inverse agonists', Molecular Simulation, 37: 2, 100 — 114
To link to this Article: DOI: 10.1080/08927022.2010.524645
URL: http://dx.doi.org/10.1080/08927022.2010.524645

Molecular Simulation
Vol. 37, No. 2, February 2011, 100–114

Taylor & Francis
Taylor & Francis Group

Molecular modelling study on human histamine H1 receptor and its applications in virtual lead identification for designing novel inverse agonists

Sundarapandian Thangapandian†, Shalini John†, Sugunadevi Sakkiah and Keun Woo Lee*

Department of Biochemistry and Division of Applied Life Science (BK21 Programme), Environmental Biotechnology National Core Research Center (EB-NCRC), Gyeongsang National University (GNU), 900 Gazwa-dong, Jinju 660701, Republic of Korea

(*Received 31 May 2010; final version received 2 September 2010*)

Human histamine H1 receptor (HHR1) is one of the G protein-coupled receptors (GPCRs) known for their constitutive activation in the absence of agonist binding. Inverse agonists are the compounds that inhibit this constitutive activity of GPCRs. HHR1 is involved in allergic reactions and is also known to be constitutively active. An updated quantitative pharmacophore model, Hypo1, has been developed using a diverse set of known HHR1 inverse agonists employing the HypoGen algorithm as implemented in Accelrys Discovery Studio 2.1. Hypo1 comprised four pharmacophore features (each one of hydrogen bond acceptor, hydrophobic, ring aromatic and positive ionisable group) along with a high correlation value of 0.944. This pharmacophore model was validated using an external test set containing 25 diverse inverse agonists and CatScramble method. Three chemical databases were screened for novel chemical scaffolds using Hypo1 as a query, to be utilised in drug design. The 3D structure of HHR1 has been constructed using human β2 adrenergic receptor. Molecular docking studies were performed with the database hit compounds using GOLD 4.1 program. The combination of all results led us to identify novel compounds to be deployed in designing new generation HHR1 inverse agonists.

Keywords: pharmacophore; homology modelling; inverse agonists; histamine H1 receptor; database screening

1. Introduction

Histamine is a biological amine synthesised from the amino acid histidine upon the enzymatic removal of its carboxyl group. This biogenic amine exerts a range of effects over various biological processes. In addition to its roles in inflammation, gastric acid secretion and as a neurotransmitter in central nervous system, the involvement of this biological amine has been observed in a variety of diseased conditions such as allergic asthma [1,2], atopic dermatitis [3,4], multiple sclerosis [5] and rheumatoid arthritis [6]. Basophils and mast cells are considered major sources of histamine and are themselves modulated upon the effects of histamine [7–9]. Histamine was discovered as a mediator of biological functions and targeting its receptors has been a well known therapeutic strategy for over 60 years. Histamine mediates its function through four receptor subtypes namely, H1, H2, H3 and H4 [10,11]. These receptors are classified under class-A G protein-coupled receptors (GPCRs), which are also known as amine class. As other GPCRs, all histamine receptor subtypes are transmembrane (TM) receptors traversing the biological membrane seven times (Figure 1). These subtypes are distinguished based on their sensitivity to specific agonists and antagonists and by their molecular weight [12–14]. Each receptor subtype is expressed in different patterns and mediates the effects distinctly. H1 receptors stimulate smooth muscle contraction and are thereby involved in allergic reactions. H2 receptors are known to have effects on gastric acid secretion, whereas H3 and H4 receptors are involved in neurotransmitter release by neurons and mast cell-mediated chemotaxis, respectively [15]. Thus, H1 receptor antagonists were developed as anti-allergic drugs. First-generation H1 antagonists such as mepyramine and diphenhydramine, though used greatly, were found to be less selective and highly sedative, because of their ability to penetrate the blood–brain barrier [16–18]. Hence, the second-generation H1 antagonists (cetirizine and acrivastine) were developed with high selectivity and less sedative potential, though some of these antagonists such as olapatadine and epinastine were non-selective [19,20]. Third-generation H1 receptor antagonists are currently in the market and are serving as effective anti-allergic drugs. A previous study reported that several H1 receptor ligands had affinity for the H4 receptor also; however, these results have not been

*Corresponding author. Email: kwlee@gnu.ac.kr
†These authors contributed equally to this work.

ISSN 0892-7022 print/ISSN 1029-0435 online

DOI: 10.1080/08927022.2010.524645
http://www.informaworld.com

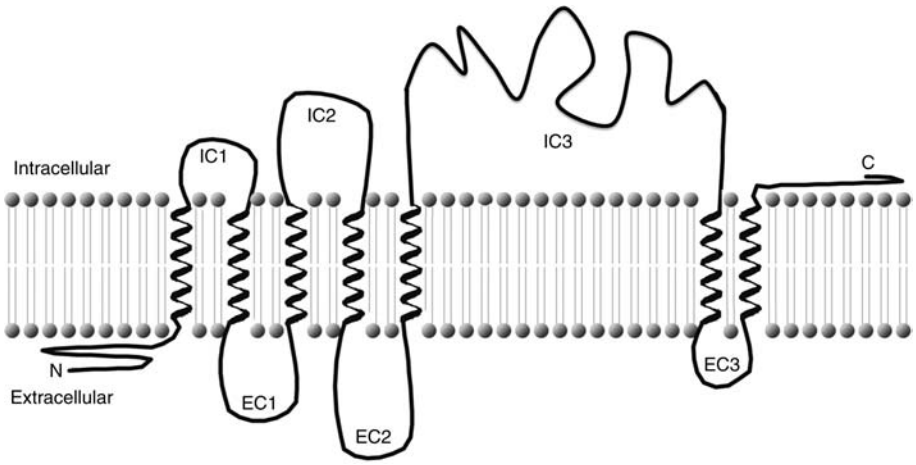

Figure 1. Schematic 2D representation of proposed structural arrangement of membrane-bound HHR1. Extracellular and intracellular parts are denoted as EC and IC, respectively. TM helices are shown in thick zigzag lines.

confirmed in other studies and should be treated with caution [21].

GPCRs are a very large family of cell surface receptors mediating extracellular (EC) signals into cells. They transduce a large variety of EC signals, including light, odorants, ions, lipids, catecholamines, neuropeptides and as well as large glycoprotein hormones [22,23]. Among the currently available drugs, 50% target GPCRs [24]. This protein family comprises seven helical TM regions traversing the membrane seven times and having three intracellular (IC) and three EC parts while the amino and carboxy terminals located in the outer and inner part of a cell. GPCRs activate their associated signal transduction pathways not only because of the agonist binding, but also in their absence leading to their constitutional activity. Receptor molecules can exist in inactive and active forms, and the neutral antagonists inhibit both forms of a receptor molecule, whereas the inverse agonist class of compounds inhibits the constitutive activity of the receptor molecule. This constitutive activity of GPCRs also has been responsible for various diseases, for instance, the constitutive activation of rhodopsin can cause congenital night blindness [25]. Many compounds once considered as GPCR antagonists are also recently being classified under inverse agonist category [26,27]. Thus, the investigation and discovery of novel GPCR inverse agonists would warrant treating a number of diseases.

In this study we have generated a highly reliable pharmacophore model, compared to the previous model, from the diverse inverse agonists of human histamine H1 receptor (HHR1). The generated pharmacophore model was further validated using a test set containing 25 compounds, followed by Fischer randomisation method. Three commercial databases were screened for the chemical compounds using the generated pharmacophore model. A homology model has been built for HHR1 and employed in the molecular docking of database-screened compounds. Finally, three compounds are listed as possible candidates for designing novel HHR1 inverse agonists.

2. Method and materials

2.1 Biological dataset collection and conformational models

Small molecular compounds with the experimental inverse agonistic properties for HHR1 receptor were taken from the literature. There were many biological assay procedures developed to assess the inverse agonistic properties of small molecules [28,29]. Compounds predicted for their inverse agonist activity using the same assay protocol were employed in pharmacophore generation [30]. A total of 43 compounds with experimental inverse agonistic properties were used in this study [30,31]; this set of compounds is an updated set of our previous set [32]. The 18 compounds with a greater diversity in terms of their chemical structures and activity values were used as the training set and rest of the compounds were utilised, as the test set, in validation of the generated pharmacophore models. Experimental inverse agonistic properties of the selected compounds were determined from the K_i values (measurement of the affinity towards the receptor) and the activity values of training-set compounds spanned over a magnitude of 10^5, i.e. 0.1–63,095.7 nM (Figure 2), which is one of the prerequisites for the Catalyst–HypoGen pharmacophore generation procedure [33]. All the compounds were drawn in Chemsketch v11 program (Advanced Chemistry Development, Inc., Toronto, Canada) and exported to Discovery Studio 2.1 (DS) program (Accelrys, Inc., San Diego, CA, USA) for further studies.

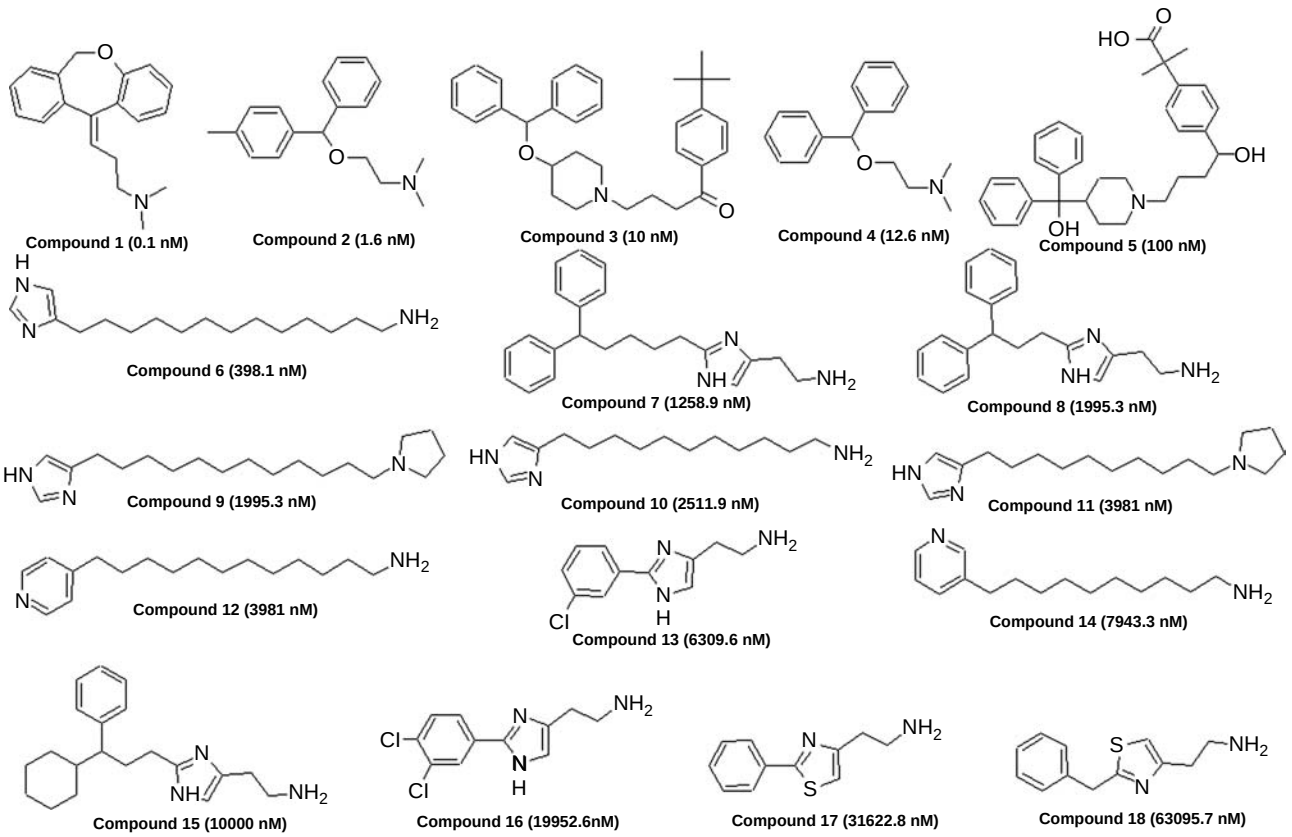

Figure 2. Training-set compounds used in pharmacophore generation with their activity (K_i) values in nanomolar concentration.

All compounds in the training set were minimised to their closest local minimum based on a modified CHARMM-like force field [34] implemented within *Confirm* module in the DS. Catalyst's pharmacophore modelling protocol HypoGen is available as the 3D QSAR Pharmacophore Generation protocol in the DS. A group of best representative conformational models for each compound in the training set has been generated by the diverse conformation generation protocol with the best conformation generation option as implemented in the DS using the Poling algorithm [35–37]. Poling explicitly promotes the conformational variation that forces similar conformers away from each other. Every training-set member is comprised of a collection of low-energy conformers that cover the conformational space accessible to the molecule within a given energy range. Best diverse conformational models for each compound were generated using an energy constraint of 20 kcal/mol and 255 as the maximum number of conformers.

All the compounds in the complete dataset were classified into four categories based on their activity (K_i) values: most active ($K_i \leq 10$ nM, ++++), active ($K_i > 10$ to ≤ 1000 nM), less active ($K_i > 1000$ to $\leq 10{,}000$ nM) and inactive ($K_i > 10{,}000$ nM).

2.2 *Pharmacophore model generation*

Prior to the generation of pharmacophore hypotheses, the feature mapping protocol of DS was employed to identify the chemical features that are present in the training-set compounds to be considered for the pharmacophore hypotheses generation. Hydrogen bond acceptor (HA), hydrogen bond donor (HD), hydrophobic (HP), positive ionisable (PI) and ring aromatic (RA) features were suggested by the feature mapping study. HypoGen module as implemented in DS was used for the generation of pharmacophore hypotheses. The uncertainty factor for each compound represents the ratio range of uncertainty in the activity value, based on the expected statistical straggling of biological data collection. Here, this factor was defined as the default value of 3. First, two most active compounds named doxepine and 4-methyl diphenhydramine with the K_i values of 0.1 and 1.585 nM, respectively, were given the principal value of 2. Both these compounds were considered most active by the HypoGen program and hence their chemical features were considered as most important during the pharmacophore hypotheses generation. The principal value was set to 0 for all other compounds in the training set. Pharmacophore hypotheses were then generated using the suggested features and

training-set compounds. Pharmacophore generation produced 10 scoring hypotheses which were exported for further calculations. The activity values of the training-set compounds are estimated using regression parameters. The relationship between the geometric fit value and the activity value is utilised for this computation. HypoGen calculates three cost values, namely fixed cost, null cost and total cost during pharmacophore generation; these are used to assess the quality of the generated pharmacophore hypotheses, thereby selecting the best one for further studies.

2.3 Pharmacophore validation

Three different validation methods have been used to validate the generated pharmacophore model. First, an external test set for testing if the pharmacophore model identifies the active compounds and predicts their activity values accurately. This external test set comprised 25 diverse compounds with a good range of HHR1 inverse agonistic activity values when compared to the training-set compounds. The selected pharmacophore hypothesis was used to predict the activity values of test-set compounds. Experimental and the predicted activity values were plotted to observe the range of correlation between them. Second, the Fischer randomisation method as available in the DS was employed to check if there is a strong correlation between the chemical structures and the biological activities and also to prove that the selected pharmacophore hypothesis is not generated by chance or random correlation. Nineteen random spreadsheets were generated to achieve a 95% confidence level. This was done by randomising the activity data associated with the training-set compounds. The same parameters set during the original pharmacophore generation were set for random pharmacophore generation. If any of the random pharmacophore hypotheses are generated with better statistical values such as high cost difference, low root mean square deviation (RMSD) and high correlation, then the original hypothesis is considered to have been generated by random correlation. The third validation method is to ensure the selectivity of the generated pharmacophore towards other histamine receptor isotypes. A small database containing antagonists of all histamine receptor isotypes was created and screened using the selected pharmacophore model as 3D query. The DS program was used to perform all the validation calculations.

2.4 Database searching and drug-likeness prediction

Pharmacophore hypotheses can be utilised as 3D queries to search chemical databases to retrieve structures that fit the hypothesis or as models to predict the potency of novel compounds. The validated pharmacophore hypothesis is used in database screening to find novel compounds from the databases. The compounds that fit all the chemical features present in the pharmacophore hypothesis are returned as hits. Three databases, namely Chembridge (CB), Maybridge (MB) and NCI2003 (NCI) containing in total 370,000 structurally diverse small molecules are used in database screening. *Ligand Pharmacophore Mapping* protocol implemented in the DS with *best flexible* search option was employed to retrieve hits. Hit compounds were subjected to rigorous drug-likeness screening to remove the compounds with undesirable properties to be drug candidates. Estimated activity and Lipinski's rule of five [38,39] were used as the primary filters along with the absorption, distribution, metabolism, excretion and toxicity (ADMET) properties. *Molecular properties* and *ADMET descriptors* protocols available in DS were used to calculate Lipinski's rule of five and ADMET properties [40].

2.5 Homology modelling

Homology model for HHR1 was built using the *Build Homology Models* protocol which builds homology models using the *Modeller* algorithm [41,42]. BLAST (blastp) search [43] as implemented in DS against Protein Data Bank (PDB) was employed to search for the proteins that are crystallographically determined and closely related to HHR1. As an update to our previous study, where squid rhodopsin was used as a template to build homology models [32], recently determined GPCR proteins, namely adenosine A2A receptor (A2AR) [44] and β2 adrenergic receptor (B2AR) [45] of human were used as possible templates from the BLAST search to build two different homology models of HHR1. The *Align Multiple Sequences* protocol of DS was utilised to align the template and the target sequences. Ten homology models were made based on each of these two templates and the final model was selected based on the overall structure quality that was calculated using PROCHECK [46,47], WhatCheck [48], ProSA-web [49,50] programs and the manual investigation of TM regions.

2.6 Molecular docking

Molecular docking methodology is a very successful strategy in drug design utilised to identify the possible binding conformation of a drug candidate prior to the developmental research [51]. In this study, molecular docking was employed to assess the binding orientations of final database hit compounds and their interactions with essential active site residues. Genetic Optimisation for Ligand Docking (GOLD) 4.1 program [52], from Cambridge Crystallographic Data Centre, UK, was employed to dock the hit compounds into the active site of HHR1.

GOLD uses a genetic algorithm for docking flexible ligands into protein binding sites with the full range of ligand conformational flexibility and partial protein flexibility [53]. 3D structural coordinates from the homology model of HHR1 were used to define the protein's active site with a radius of 10 Å around the ligand copied from the template. The default value of 3 for early termination option was changed to 5 to call the program to quit or skip the genetic optimisation if any five conformations of a particular compound are within the RMSD value of 1.5 Å. All other parameters were kept at their default values.

3. Results and discussion

3.1 Pharmacophore modelling

A training set of 18 compounds, which are diverse in their structures and activity values, is used in pharmacophore generation. This training set comprises a new set of diverse compounds when compared to our previous study. The activity values of these compounds are reported as K_i values (as a measurement of affinity to the receptor) spanning from 0.1 to 63,095.7 nM with a magnitude of 10^5. Every compound in the training set must provide some new structural information to obtain a good model in terms of predictive ability and statistical significance. As suggested by the *Feature Mapping* protocol HA, HD, HP, PI and RA features were selected to be used in pharmacophore generation. The minimum and maximum number for every pharmacophoric feature was set to 0 and 5, respectively, and thereby not forcing the algorithm to generate hypotheses with a certain number of particular chemical feature. Pharmacophore hypotheses were computed and the top 10 hypotheses were exported for further studies. Seven of ten generated pharmacophore hypotheses of the following chemical features were made: HA, HP, PI and RA functions whereas others possessed more HP features instead of either RA or both PI and RA. Thus, these four chemical features could effectively map all the chemical features of the training-set compounds. Hypo1 has been made of each one of HA, HP, PI and RA functionalities (Figure 3). Previous studies have also reported similar pharmacophore models for HHR1 antagonists [53]. As reported earlier, the distance between the PI function (generally the basic nitrogen atom) and the aromatic part of the ligand ought to be around 6 Å [32,54]. In our model, it is 6.267 Å between PI and RA, and 6.361 Å between PI and HP features, respectively. These observations support our pharmacophore model for its reasonable spatial arrangements. A significant hypothesis must possess the large difference between null and fixed cost values [55]. In this study, the null cost value of the top 10 hypotheses is 154.908, the fixed cost value is 68.612 and the configuration cost value is 6.943. In simple terms, there should be a large difference between the fixed cost and the null cost with a value of 40–60, which would imply a 75–90% probability for correlating the experimental and estimated activity data. The total cost of any hypothesis should be close to the fixed cost for a good model. In our study, all 10 hypotheses have a total cost close to the fixed cost value. The difference between the fixed cost and the null cost is 86.296 bits and may lead to a meaningful pharmacophore model. The cost difference between the total cost of all 10 hypotheses and the null hypothesis varies between 69 and 45 bits. However, first two hypotheses scored cost differences more than 60 and hence greater than 90% possibility of representing a true correlation between the experimental and estimated activity data for these hypotheses (Table 1). The RMSD indicates the quality of prediction for the training set. The RMSD of all 10 hypotheses ranged from 1.049 to 2.124 Å. Besides this cost analysis, the most obvious method to validate the hypotheses is testing the ability to predict the activity of the training-set compounds. First hypothesis (Hypo1) has scored better and has statistically significant values such as high correlation coefficient which represents the good correlation between the experimental and estimated activity values, larger cost difference and low RMSD. Configuration cost should be less than 17 for a

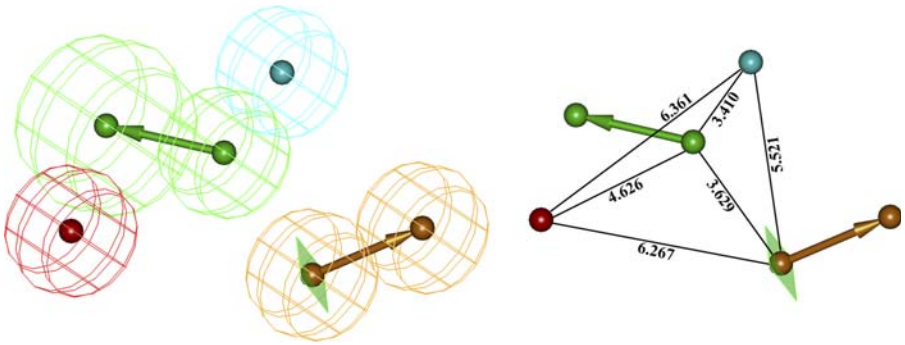

Figure 3. The best pharmacophore model Hypo1 shown with its inter-feature distances. Green, cyan, brown and red colours indicate HA, HP, RA and PI features, respectively (colour online).

Table 1. Statistical output for the pharmacophore generation calculation.

Hypothese	Total cost	Cost difference[a]	RMSD	Error cost	Correlation	Features
1	85.706	69.202	1.049	70.449	0.955	HA HP PI RA
2	89.679	65.229	1.238	74.332	0.933	HA HP PI RA
3	98.319	56.589	1.625	84.299	0.874	HA HP HP PI
4	98.901	56.007	1.769	88.697	0.840	HA HP PI RA
5	100.207	54.701	1.805	89.878	0.833	HA HP PI RA
6	101.326	53.582	1.862	91.739	0.819	HA HP HP PI
7	102.74	52.168	1.899	93.003	0.812	HA HP PI RA
8	105.82	49.088	1.979	95.789	0.794	HA HP PI RA
9	107.054	47.854	2.007	96.785	0.788	HA HP PI RA
10	109.402	45.506	2.124	101.147	0.755	HA HP HP HP

Null cost = 154.908; fixed cost = 68.612; config cost = 6.943; HA, hydrogen bond acceptor; HP, hydrophobic; PI, positive ionisable; RA, ring aromatic.
[a]Cost difference = null cost − total cost.

significant hypothesis. Hypo1 was generated with a configuration value of 6.973. The overlay of the most active compound **1**, doxepine, shows that it mapped well upon all the features of the pharmacophore model (Hypo1). The first and the third rings of the fused ring system of doxepine mapped onto the HP and RA features whereas the oxygen atom present in the middle ring mapped over the HA feature. The tertiary amino group present in compound **1** mapped over the PI feature of Hypo1 (Figure 4(a)). Thus, the activity of compound **1** was estimated very closely to its experimental activity by the best pharmacophore model, Hypo1. It is reported that the PI group of any HHR1 antagonists is significant to interact with the catalytically important Asp107 residue in the active site [56]. Least active compound **18** in the training set mapped three of the four features present in Hypo1, missing the RA feature. Phenyl and pyrrole rings mapped over the HP and HA features while the primary amino group enabled the mapping over PI feature of Hypo1 (Figure 4(b)). Top five compounds in the training set could map over all the chemical features of Hypo1 and the remaining compounds mapped at least three features. This overlay comparison of the most and the least active compounds provides a clue that the RA group present in most active compounds could be important and thereby indicating that HP interactions at the active site add value to the ligand–protein interaction. Hypo1 has predicted most of the activity values considerably for the training set compounds except one compound each in most active, active and less active category (Table 2), with the correlation value (r) of 0.955 (Figure 5).

3.2 *Pharmacophore model validation*

The predictive power of Hypo1 was analysed using three different methods: (1) test set prediction (2) Fischer's randomisation test and (3) selectivity analysis. A test set containing 25 compounds with a high range of activity with diverse structures compared to the training set compounds was used. The best conformation for every test-set compound was generated and mapped upon the Hypo1 model to predict the fit and estimated activity values. *Best flexible search* option of the *Ligand Pharmacophore Mapping* protocol available in the DS has been used in this test set validation process. Estimated activity values of members of test set were predicted well to their experimental activity with low error values (Table 3). Furthermore, Hypo1 was used to perform a regression analysis with the test set compounds in order to check the predictive power of this model. Linear regression of the estimated activities vs. the experimental activities of test-set compounds showed a correlation value

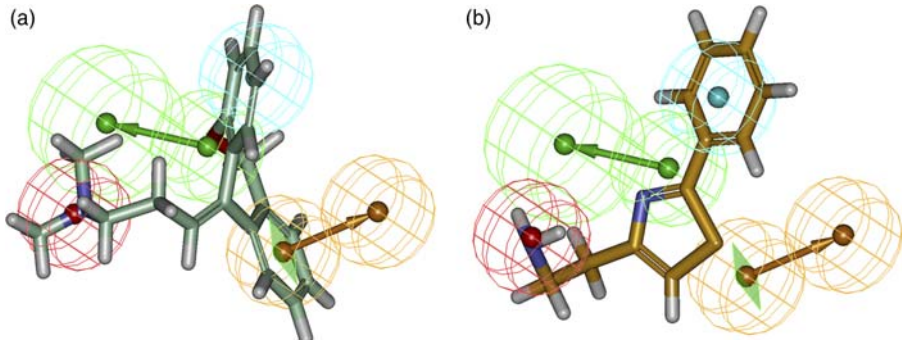

Figure 4. Overlay of the most active compound **1** (a) and least active compound **18** (b) of the training set upon Hypo1.

Table 2. Activity estimation for training-set compounds based on Hypo1.

Compound	Fit value	K_i (nM)		Error[a]	Activity scale[b]	
		Experimental	Estimated		Experimental	Estimated
1	12.13	0.1	0.8	8	++++	++++
2	11.28	1.6	5.7	3.6	++++	++++
3	10.18	10	71	7.1	++++	+++
4	10.94	13	13	−1	+++	+++
5	10.71	100	21	−4.7	+++	+++
6	8.91	400	1300	3.4	+++	++
7	9.01	1300	1100	−1.2	++	++
8	8.53	2000	3200	1.6	++	++
9	8.58	2000	2900	1.4	++	++
10	8.74	2500	2000	−1.3	++	++
11	8.84	4000	1600	−2.5	++	++
12	9.10	4000	870	−4.6	++	++
13	7.72	6300	21,000	3.3	++	+
14	8.70	7900	2200	−3.7	++	++
15	8.31	10,000	5400	−1.9	++	++
16	7.94	20,000	13,000	−1.6	+	+
17	7.58	32,000	29,000	−1.1	+	+
18	7.97	63,000	12,000	−5.4	+	+

[a] A positive value indicates that the estimated activity is higher than the experimental activity and a negative value indicates that the estimated activity is lesser than the experimental activity. [b] Activity scale: most active, ++++ (IC50: $K_i \leq 10$ nM); active, +++ (IC50: $10 < K_i \leq 1000$ nM); less active, ++ (IC50: $1000 < K_i \leq 10{,}000$ nM); inactive, + (IC50: $K_i > 10{,}000$ nM).

of 0.946 (Figure 5). This result supports the validity of the statistically significant HypoGen hypothesis in predicting the affinity for HHR1. In addition, Fischer's randomisation method was applied to check if the pharmacophore model, Hypo1, is generated as result of random correlation of activity values of training set compounds. To achieve the 95% confidence level, 19 random spreadsheets were generated by HypoGen. The data of randomisation test clearly showed that none of the randomly generated models showed a better statistical significance than Hypo1 (Table 4). Six of 19 random hypotheses have scored correlation values higher than 0.8 but none have scored better RMSD and fixed cost values than Hypo1.

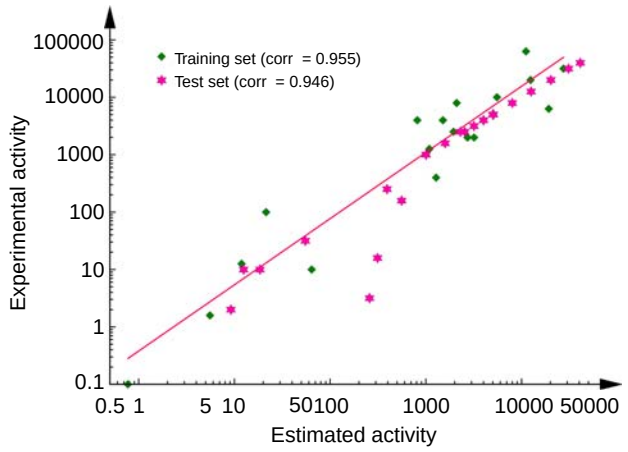

Figure 5. Correlation plot between the experimental and estimated activities of the training and test set compounds.

A selectivity analysis was conducted to confirm the selectivity of the best pharmacophore model, Hypo1. A small database containing antagonists of all histamine receptor isotypes was created and screened using Hypo1 as a 3D query. *Ligand Pharmacophore Mapping* protocol with *best conformation generation* option was used to screen this small database. From the result, 87.50% of the H1 antagonists were retrieved whereas only 13.73, 9.09 and 30.43% of H2, H3 and H4 antagonists, respectively, were retrieved (Table 5). This confirms the selective nature of the generated pharmacophore model towards HHR1. Thus, the validated pharmacophore model could be used to perform virtual screening as a powerful tool to retrieve new potent molecules for designing HHR1 inverse agonists. In our study, the validated pharmacophore model was used to search CB, MB and NCI databases consisting of 370,000 compounds. The query returned 4317, 6398 and 8956 hits from CB, MB and NCI databases, respectively, and they were all selected and subjected to various screening steps by restricting the estimated activity less than 2 nM, Lipinski's rule of five and ADMET properties. These screenings were used to avoid the non-drug-like compounds being carried to the next step in the computer-aided drug discovery research. A Lipinski-positive compound should meet the following: (1) a molecular weight less than 500, (2) number of hydrogen bond donors less than 5, (3) number of HAs less than 10 and (4) an octanol/water partition coefficient (Log *P*) value less than 5. As a result, a total of 63 compounds (22 from CB, 37 from MB and 4 from NCI) were retained (Figure 6). These compounds were then

Table 3. Activity estimation of test set compounds based on Hypo1.

Compound	Fit value	K_i (nM)		Error[a]	Activity scale[b]	
		Experimental	Estimated		Experimental	Estimated
19	11.077	1.995	9.187	4.61	++++	++++
20	9.628	3.162	257.969	81.58	++++	+++
21	10.773	10	18.491	1.85	++++	+++
22	10.944	10	12.476	1.25	++++	+++
23	9.545	15.849	312.844	19.74	+++	+++
24	10.299	31.623	55.033	1.74	+++	+++
25	9.293	158.489	558.624	3.52	+++	+++
26	9.446	251.189	392.673	1.56	+++	+++
27	9.038	1000	1004.78	1.01	+++	++
28	9.039	1000	1003.05	1	+++	++
29	8.839	1584.89	1589.29	1.01	++	++
30	8.635	2511.89	2543.71	1.01	++	++
31	8.678	2511.89	2303.82	−1.09	++	++
32	8.538	3162.28	3177.27	1.01	++	++
33	8.438	3981.07	3998.88	1.01	++	++
34	8.438	3981.07	3999.28	1.02	++	++
35	8.437	3981.07	4004.36	1.04	++	++
36	8.334	5011.87	5080.92	1.04	++	++
37	8.340	5011.87	5006.62	−1.01	++	++
38	8.137	7943.28	7989.59	1.04	++	++
39	7.940	12589.3	12581.1	−1	+	+
40	7.940	12589.3	12582.6	−1	+	+
41	7.734	19952.6	20224.7	1.03	+	+
42	7.550	31622.8	30921.6	−1.02	+	+
43	7.427	39810.7	40996.3	1.03	+	+

[a] A positive value indicates that the estimated activity is higher than the experimental activity and a negative value indicates that the estimated activity is lesser than the experimental activity. [b] Activity scale: most active, ++++ (IC50: $K_i \leq 10$ nM); active, +++ (IC50: $10 < K_i \leq 1000$ nM); less active, ++ (IC50: $1000 < K_i \leq 10{,}000$ nM); inactive, + (IC50: $K_i > 10{,}000$ nM).

Table 4. Comparison of statistical values of random pharmacophore hypotheses with Hypo1.

Trial no.	Total cost	Fixed cost	RMSD	Correlation	Configuration cost
Results for unscrambled					
Hypo1	85.706	69.202	1.049	0.955	6.943
Results for scrambled					
Trial 1	120.910	76.897	2.066	0.782	15.228
Trial 2	135.645	75.726	2.465	0.670	14.06
Trial 3	154.908	60.545	3.238	0.000	0.000
Trial 4	117.573	78.423	1.975	0.798	16.753
Trial 5	127.896	75.161	2.263	0.737	13.491
Trial 6	113.563	75.023	1.882	0.827	13.353
Trial 7	112.777	75.019	1.904	0.818	13.349
Trial 8	120.729	68.589	2.385	0.678	6.919
Trial 9	135.054	74.955	2.525	0.635	13.286
Trial 10	154.908	60.545	3.238	0.000	0.000
Trial 11	114.290	82.145	1.854	0.821	20.475
Trial 12	154.908	60.545	3.238	0.000	0.000
Trial 13	135.131	75.151	2.555	0.617	13.481
Trial 14	123.615	74.969	2.259	0.722	13.299
Trial 15	104.082	75.161	1.657	0.864	13.491
Trial 16	140.740	74.949	2.704	0.550	13.279
Trial 17	121.939	75.797	2.017	0.810	14.127
Trial 18	110.331	77.480	1.854	0.822	15.810
Trial 19	128.211	73.488	2.347	0.705	11.818

Table 5. Selectivity analysis between histamine receptor isotypes.

	Compounds		
Isotype	Total	Screened	Percentage (%)
H1	48	42	87.50
H2	51	7	13.73
H3	44	4	9.09
H4	46	14	30.43

subjected to molecular docking study in order to observe the essential ligand–protein binding interactions at the active site. Since the crystal structure of HHR1 is not available yet, we have constructed the model structure by homology modelling method using different templates in the DS and used the best model in molecular docking calculations.

3.3 Homology modelling of HHR1 structure

Structure modelling of HHR1 has been a great concern since the first crystal structure of GPCR was determined. Many research groups have obtained homology models for HHR1 [56,57]. In the beginning, it was bacterial rhodopsin used as the template for the modelling, followed by bovine rhodopsin (PDB ID: 1F88 with 2.8 Å resolution). In our previous work, we have used the crystal structure of squid rhodopsin (PDB ID: 2Z73, 2.5 Å resolution) as the template to model HHR1 3D structure [32]. Rhodopsin template was lacking the information for the long intracellular part (IC3) that is present in HHR1 to bind the G protein and takes part in transducing the signal. Since the crystal structures of human proteins from GPCR family were recently crystallised, it is necessary to rebuild the HHR1 and use it in molecular-docking studies. There are some studies on various GPCR proteins that have made comparison of the models that was built using the recently crystallised structures with the previously used rhodopsin structures [58]. As a result, the studies have mentioned that the recent human GPCR structures could be used to build more reliable 3D structures than others. In this study, crystal structures of A2AR and B2AR of human were used individually to construct the homology model for HHR1. The quality of the homology models was compared with each other as well as with the results of our previous study (Table 6). The *Build homology models* protocol implemented in the DS was used to construct the homology models. Ten homology models using each template were built and their stereochemical quality was checked using PROCHECK, WhatCheck and ProSA results. These human GPCRs also possessed the equivalent part to the G protein-binding region that was missing in the rhodopsin structure. The alignment was carefully investigated, especially in TM regions for their integrity and we found that all of the critical structural elements known to be involved in the binding of its natural substrate, histamine, are intact. In addition to this, the PROCHECK analysis was performed to validate the reliability of the model structures. The percentage of residues predicted in the disallowed regions was acceptable for all models. Goodness factor (*G* factor), which represents how normal or unusual the residue's location is on the Ramachandran plot, was calculated for all the models. Analyses of bad contacts, bond lengths, bond angles, *Z* scores from Ramachandran plot and ProSA prediction concluded that model 1 is a reliable model for further studies. Based on the stereochemical reliability, the homology model generated using human B2AR was selected to be used in molecular docking study. The sequence alignment between HHR1 and human B2AR showed 25.3% identity and 50.2% similarity (Figure 7). PROCHECK predicted 99.5% (91.1% of residues in the most favoured regions, 7.2% of residues in the additional allowed regions and 1.2% of residues in the generously allowed regions) of total residues (467 residues) of the model structure present in the allowed regions having only two amino acids in the disallowed region. We have modelled HHR1 with a high accuracy of 91.1% in the most favoured regions using the recently crystallised high resolution template, whereas it was 86.2% in our previous study and the reliability of the model was confirmed with various analyses. Thus, the model built using human B2AR could be used further in

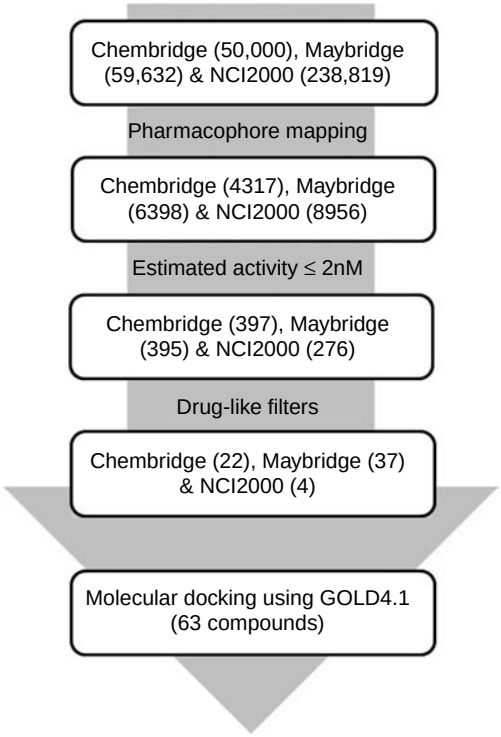

Figure 6. Database screening details using Hypo1 as a 3D query.

Table 6. Main geometric parameters of the three HHR1 models built using different templates.

HHR1 models	Template	Ramachandran plot						M/c bond lengths (%)	M/c bond angles (%)	Planar groups (%)	ProSA *Z*-score
		Core (%)	Allow (%)	Gener (%)	Disall (%)	Bad contacts	*G* factor[a]				
1	Human β2 adrenergic receptor	91.1	7.2	1.2	0.5	12	−0.02	98.6	93.5	99.4	−3.84
2	Human A2A adenosine receptor	86.7	12.4	0.5	0.5	26	−0.18	98.1	90.0	98.8	−3.4
3	Squid rhodopsin	86.2	10.9	1.5	1.5	138	−0.09	96.4	94.3	79.5	−2.92

[a] *G* factor – goodness factor and this value should be > -0.5 for a good model.

the molecular docking study. Constructed model was overlaid upon the template protein and the RMSD observed between the constructed model and the template was 0.210 Å, which forecasted the reliability of the model (Figure 8). Ramachandran plot and *Z*-score plot of ProSA analysis are shown in Figure 9. Comparison of the selected HHR1 model with our previous model (data not shown) revealed that the second TM helix was not constructed completely in rhodopsin-based model, though the alignment with rhodopsin provided the equivalent TM region information. But, in the current model, all seven TM helices were completely constructed without any distortion in their structures.

3.4 Molecular docking

Database hits, along with the training set compounds were docked into the active site of homology-modelled HHR1. W158, F432 and F435 are the residues that were proved to take part in antagonist binding [56] and arranged in favourable positions to form a lipophilic cavity. The other aromatic residues, which are potential lipophilic interaction points, were found in TM3 (D107, Y108), at the end of EC3 (F184), in TM5 (F190, F199) and in TM6 (F424, W428, W431). K191 in TM5 was found in the internal side of the receptor, and seemed to be able to create an ionic interaction with the carboxylate group of zwitterionic inhibitors [56,59]. These residues were considered while creating the binding site for the docking process.

All docking calculations were performed using the GOLD 4.1 program. The structural observation and comparison of the 3D structures of the current model with previous model differed from each other. The total deviation between two models is 13.23 Å and particularly the active site residues deviated to a greater extent. This deviation was very much observable at the fourth TM helix and the consequent loop, where W158, F184, F190 and K191 residues are located. These residues were predicted away from the active site of our previous model, but predicted close to the active site in our current model. Overall, one side of the active site of the receptor was formed by a set of aromatic amino acids (F424, W428, Y431, F432 and F435), making it highly HP in nature, while a blend of aromatic (Y108 and W158), negatively charged (D107 and E177) and polar uncharged (S111) amino acids form the other side. This arrangement of amino acids confirms that the inhibitor has to bind in such a way that its PI and aromatic groups are positioned towards the negatively charged amino acid and HP part of the catalytic site, respectively. Our molecular docking studies resulted in the same positioning of ligands in the active site. The binding site with 10 Å radius was defined using the crystal structure-bound ligand present in the crystal structure of human B2AR. This ligand was copied

Figure 7. Sequence alignment between target (HHR1) and template (human B2AR, PDB ID: 2RH1) sequences. The start and end of every TM helix is marked with red block forward and backward arrows. EC, extracellular; IC, intracellular; TM, transmembrane.

from the template structure during homology modelling. Top 20 conformations of every compound were allowed to be saved. Two most active compounds, namely doxepine and 4-methyl diphenhydramine in the training set have scored GOLD fitness scores of 49.604 and 52.912, respectively, and generated strong hydrogen bond interactions with Tyr108, and its two aryl groups were positioned in the lipophilic cavity, formed by other active site amino acids (Figure 10(a)). The 'GOLD score' scoring function was selected over the other available scoring functions such as ChemScore, Astex Statistical Potential or piecewise linear potential for the molecular-docking calculations, as the 'GOLD score' is a widely used and majorly validated scoring function upon a huge dataset [52]. Moreover, this scoring function has performed better for the training-set compounds of this study. Twenty-seven compounds have scored the GOLD fitness score greater than 50 and they were considered for further evaluation. The compound named AW01220 from MB database has scored the highest GOLD score of 71.584 and formed hydrogen bond interactions with the essential amino acids, D107 and F184 (Figure 10(b)). This compound has scored a HypoGen estimated activity value of 0.449 nM. Compound 25341 from CB database which scored an estimated activity value of 1.052 nM has also scored a GOLD fitness score of 65.753 and formed a hydrogen bond network with D107, Y108, W158 and F184 (Figure 10(c)). Finally, another compound named KM11105, also from MB database, scored a GOLD fitness score of 62.068 and formed hydrogen bond interactions with Y108, W158 and F184, along with an estimated activity value of 0.99 nM (Figure 10(d)).

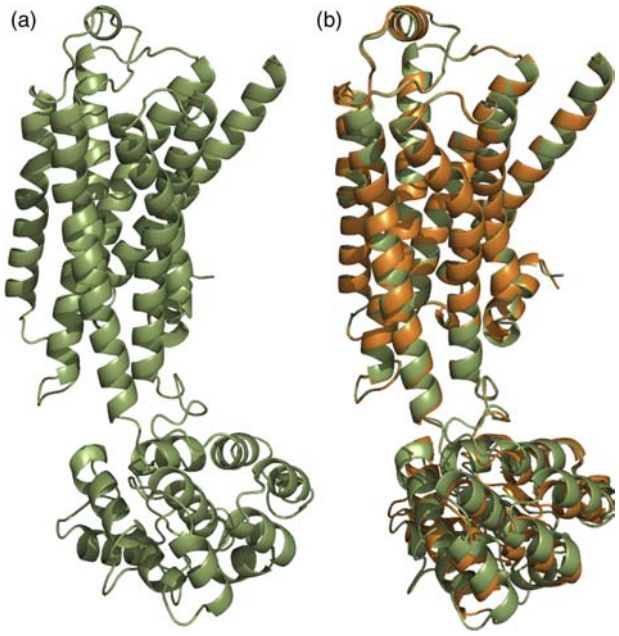

Figure 8. Results of homology modelling. (a) Homology model of HHR1 and (b) its overlay with the template structure.

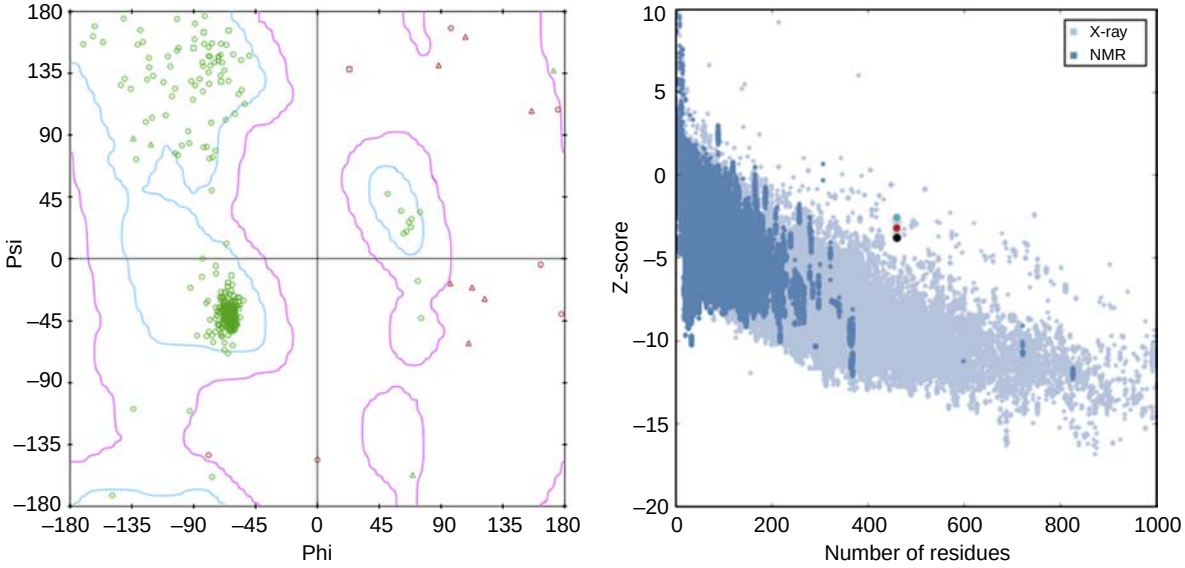

Figure 9. Plots explaining the stereochemical quality of the selected homology model of HHR1. Ramachandran plot (left) showing the residues in allowed (green spots) and disallowed (red spots) regions. ProSA plot (right) displaying the *Z*-score for model 1 (black spot), model 2 (red spot) and model 3 (green spot) (colour online).

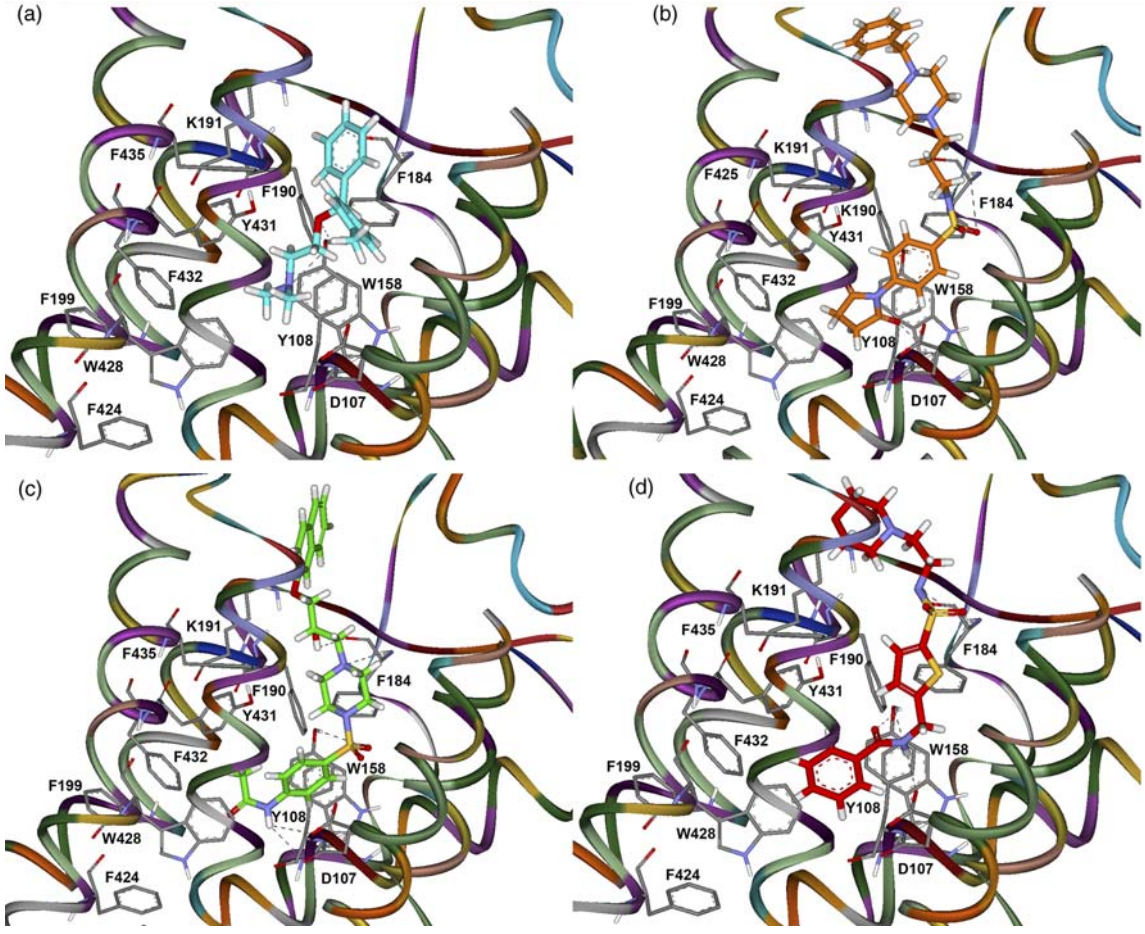

Figure 10. Molecular-docking results using GOLD 4.1. (a) 4-Methyl diphenhydramine, cyan colour (b) AW01220, orange colour (c) Compound 25341, green colour and (d) KM11105, red colour (colour online). HHR1 structure is represented in ribbon form. Hydrogen bonds are shown in dotted lines. Only polar hydrogens are shown for clarity.

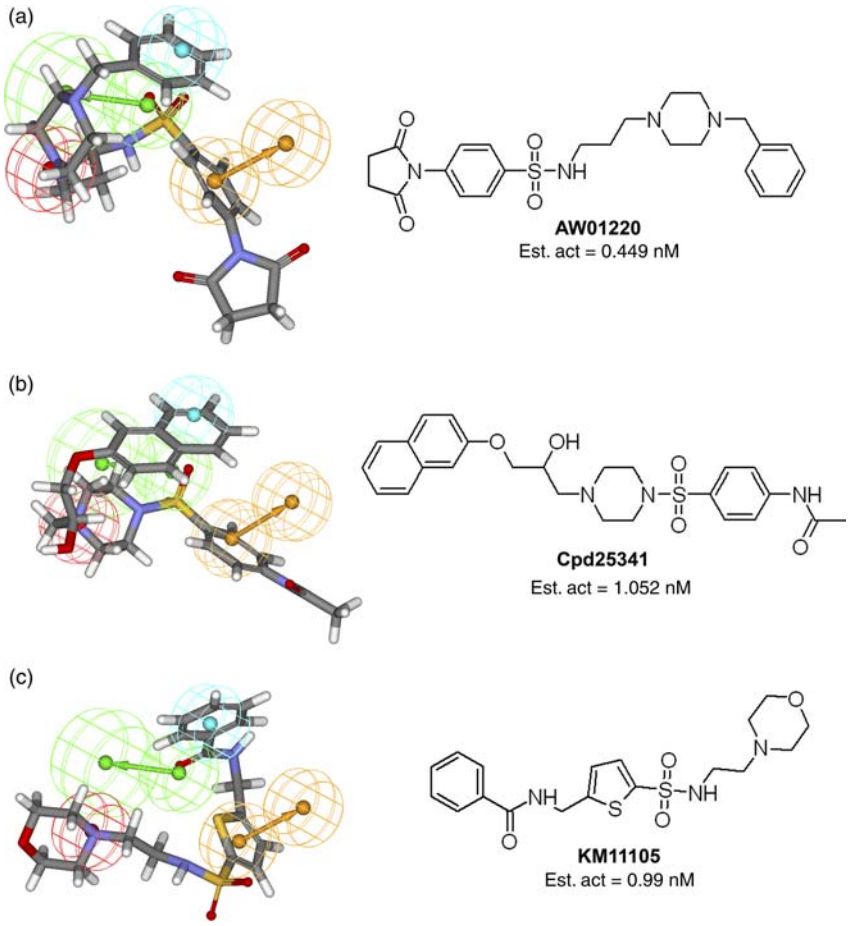

Figure 11. Overlay of final hit compounds on Hypo1 and their corresponding 2D molecular structures with estimated activity values (a) AW01220, (b) Compound 25341 and (c) KM11105.

These three final compounds have scored better results with respect to all properties such as estimated activity, drug-like properties, GOLD fitness score and essential hydrogen bond interactions with the active site residues. These compounds are of different scaffolds, and the novelty search using *SciFinder Scholar* [60,61] has confirmed that these compounds were not reported earlier for HHR1 antagonistic properties. Figure 11 shows the final hit compounds with their overlay on Hypo1 and their 2D structures.

4. Conclusions

Histamine binds with its receptors and exerts its physiological effects through them. Among these receptors, HHR1 is responsible for allergic reactions. This receptor is classified as one of the amino class (class A) of GPCRs and constitutively active, i.e. they are active before the binding of an agonist. Many of its antagonists are found to inhibit the constitutional activity of this receptor prior to its activation upon agonist binding, which led to the reclassification of these antagonists as inverse agonists. These inverse agonists are much selective towards the inactive conformation of the receptor rather than its active conformation. Thus, the novel inverse agonists would be helpful in the treatment of various allergic conditions. As an effort towards this, we have developed an updated pharmacophore model, compared to our previous study, with a diverse set of known inverse agonists. A pharmacophore model, Hypo1, was selected based on its statistical significance and validated using three different methods which confirmed its predictive ability on new compounds and the selectivity. This validated pharmacophore model was further used in database searching to identify novel scaffolds to be used in HHR1 drug designing. Resulted compounds were subjected to various filters to select the compounds with the estimated activity value less than 2 nM and drug-like properties. As it is difficult to crystallise any GPCR protein, the crystal structure of HHR1 is also not crystallised yet. Thus, two updated homology models, compared to our previous study, were constructed based on human A2AR and

human B2AR, separately. Finally, based on the stereochemical quality of the constructed models, the model based on human B2AR was selected and utilised in the molecular docking of database-hit compounds. Combining the results from database screening, homology modelling and molecular docking, three novel compounds with different scaffolds were reported as possible virtual lead candidates in HHR1 inverse agonist designing. The novelty of these final compounds was conformed through the novelty analysis using the *SciFinder Scholar* search.

Acknowledgements

All authors were supported by a scholarship from the BK21 Program, the Ministry of Education, Science and Technology (MEST), Korea; this work was supported by the Basic Science Research Program (2009-0073267) and Environmental Biotechnology National Core Research Center Program (20090091489) through the National Research Foundation of Korea (NRF) funded by MEST.

References

[1] D.H. Broide, G.J. Gleich, A.J. Cuomo, D.A. Coburn, E.C. Federman, L.B. Schwarte, and S.I. Wasserman, *Evidence of ongoing mast cell and eosinophil degranulation in symptomatic asthma airway*, J. Allergy Clin. Immunol. 88 (1991), pp. 637–648.

[2] S.E. Wenzel, A.A. Fowler, and L.B. Schwartz, *Activation of pulmonary mast cells by bronchoalveolar allergen challenge.* In vivo *release of histamine and tryptase in atopic subjects with and without asthma*, Am. Rev. Respir. Dis. 137 (1988), pp. 1002–1008.

[3] H.H. Johnson, Jr, G.A. Deoreo, W.P. Lascheid, and F. Mitchell, *Skin histamine levels in chronic atopic dermatitis*, J. Invest. Dermatol. 34 (1960), pp. 237–238.

[4] L. Juhlin, *Localization and content of histamine in normal and diseased skin*, Acta Derm. Venereol. 47 (1967), pp. 383–391.

[5] L. Tuomisto, H. Kilpelainen, and P. Riekkinen, *Histamine and histamine-N-methyltransferase in the CSF of patients with multiple sclerosis*, Agents Actions. 13 (1983), pp. 255–257.

[6] D.B. Frewin, L.G. Cleland, J.R. Jonsson, and P.W. Robertson, *Histamine levels in human synovial fluid*, J. Rheumatol. 13 (1986), pp. 13–14.

[7] C.L. Hofstra, P.J. Desai, R.L. Thurmond, and W.P. Fung-Leung, *Histamine H4 receptor mediates chemotaxis and calcium mobilization of mast cells*, J. Pharmacol. Exp. Ther. 305 (2003), pp. 1212–1221.

[8] U. Lippert, M. Artuc, A. Grützkau, M. Babina, S. Guhl, I. Haase, V. Blaschke, K. Zachmann, M. Knosalla, P. Middel, S. Krüger-Krasagakis, and B.M. Henz, *Human skin mast cells express H2 and H4, but not H3 receptors,*, J. Invest. Dermatol. 123 (2004), pp. 116–123.

[9] V. Godot, M. Arock, G. Garcia, F. Capel, C. Flys, M. Dy, D. Emilie, and M. Humbert, *H4 histamine receptor mediates optimal migration of mast cell precursors to CXCL12*, J. Allergy Clin. Immunol. 120 (2007), pp. 827–843.

[10] B. Leader, Q.J. Baca, and D.E. Golan, *Protein therapeutics: A summary and pharmacological classification*, Nat. Rev. Drug Discov. 7 (2008), pp. 21–39.

[11] I.J.P. de Esch, R.L. Thurmond, A. Jongejan, and R. Leurs, *The histamine H4 receptor as a new therapeutic target for inflammation*, Trends Pharmacol. Sci. 26 (2005), pp. 462–469.

[12] R.E. Brown, D.R. Stevens, and H.L. Haas, *The physiology of brain histamine*, Prog. Neurobiol. 63 (2001), pp. 637–672.

[13] T. Oda, N. Morikawa, Y. Saito, Y. Masuho, and S. Matsumoto, *Molecular cloning and characterization of novel type of histamine receptor preferentially expressed in leukocytes*, J. Biol. Chem. 275 (2000), pp. 36781–36786.

[14] R. Leurs, M.S.R. Pena, R.A. Bakker, A.E. Alewijnse, and H. Timmerman, *Constitutive activity of G protein coupled receptors and drug action*, Pharm. Acta Helv. 74 (2000), pp. 327–331.

[15] W.A. Fogel, W. Wagner, K. Sasiak, and A. Stasiak, *The role of histamine in experimental ulcerative colitis in rats*, Inflamm. Res. 54 (2005), pp. S68–S69.

[16] M. Kakiuchi, T. Ohashi, K. Musoh, K. Kawamura, K. Morikawa, and H. Kato, *Studies on the novel antiallergic agent HSR-609: Its penetration into the central nervous system in mice and guinea pigs and its selectivity for the histamine H1-receptor*, Jpn. J. Pharmacol. 73 (1997), pp. 291–298.

[17] B.C. Sangalli, *Role of the central histaminergic neuronal system in the CNS toxicity of the first generation H1-antagonists*, Prog. Neurobiol. 52 (1997), pp. 145–157.

[18] M.J. Welch, E.O. Meltzer, and F.E.R. Simons, *Histamine and H1-Antihistamines in Allergic Disease*, F.E.R. Simons, ed., 2nd ed., Marcel Dekker, New York, 2002, pp. 337–388.

[19] F.E. Simons and K.J. Simons, *Clinical pharmacology of new histamine H receptor antagonists*, Clin. Pharmacokinet. 36 (1999), pp. 329–352.

[20] G.M. Walsh, L. Annunziato, N. Frossard, K. Knol, S. Levander, J.M. Nicolas, M. Taglialatela, M.D. Tharp, J.P. Tillement, and H. Timmerman, *New insights into the second generation antihistamines*, Drugs 61 (2001), pp. 207–236.

[21] L.B. Hough, *Genomics meets histamine receptors: New subtypes, new receptors*, Mol. Pharmacol. 59 (2001), pp. 415–419.

[22] J. Bockaert and J.P. Pin, *Molecular tinkering of G protein-coupled receptors: An evolutionary success*, EMBO J. 18 (1999), pp. 1723–1729.

[23] N. Tuteja, *Signaling through G protein coupled receptors*, Plant Signal. Behav. 4 (2009), pp. 942–947.

[24] N.D. Matthew and D.R. Flower, In silico *identification of novel G protein coupled receptor*, Methods Mol. Biol. 528 (2009), pp. 25–36.

[25] Y.X. Tao, *Constitutive activation of G protein-coupled receptors and diseases: Insights into mechanisms of activation and therapeutics*, Pharmacol. Ther. 120 (2008), pp. 129–148.

[26] S. Parra and R.A. Bond, *Inverse agonism: From curiosity to accepted dogma, but is it clinically relevant?* Curr. Opin. Pharmacol. 7 (2007), pp. 146–150.

[27] F. Monczor, N. Fernandez, B.L. Legnazzi, M.E. Riveiro, A. Baldi, C. Shayo, and C. Davio, *Histamine H1-receptor activation of nuclear factor-κB: Roles for Gβγ- and Gαq/11-subunits in constitutive and agonist-mediated signaling*, Mol. Pharmacol. 64 (2003), pp. 512–520.

[28] C.P. Fitzsimons, F. Monczor, N. Fernandez, C. Shayo, and C. Davio, *Mepyramine, a histamine H1 receptor inverse agonist, binds preferentially to a G protein-coupled form of the receptor and sequesters G protein*, J. Biol. Chem. 279 (2004), pp. 34431–34439.

[29] R.A. Bakker, K. Wieland, H. Timmerman, and R. Leurs, *Constitutive activity of the histamine H1 receptor reveals inverse agonism of histamine H1 receptor antagonists*, Eur. J. Pharmacol. 387 (2000), pp. R5–R7.

[30] R.A. Bakker, S.B.J. Schoonus, M.J. Smit, H. Timmerman, and R. Leurs, *Histamine H1-receptor activation of nuclear factor-κB: Roles for Gβγ- and Gαq/11-subunits in constitutive and agonist-mediated signaling*, Mol. Pharmacol. 60 (2001), pp. 1133–1142.

[31] M. Govoni, R.A. Bakker, I. van de Wetering, M.J. Smit, W.M. Menge, H. Timmerman, S. Elz, W. Schunack, and R. Leurs, *Synthesis and pharmacological identification of neutral histamine H1-receptor antagonists*, J. Med. Chem. 46 (2003), pp. 5812–5824.

[32] S. Thangapandian, N. Krishnamoorthy, S. John, S. Sakkiah, P. Lazar, Y. Lee, and K.W. Lee, *Pharmacophore modeling, virtual screening and molecular docking studies for identification of new inverse agonists of human histamine H1 receptor*, Bull. Korean Chem. Soc. 31 (2010), pp. 52–58.

[33] Y.D. Chen, Y.J. Jiang, J.W. Zhou, Q.S. Yu, and Q.D. You, *Identification of ligand features essential for HDACs inhibitors by pharmacophore modeling*, J. Mol. Graph. Model. 26 (2008), pp. 1160–1168.

[34] B.R. Brooks, R.E. Bruccoleri, B.D. Olafson, D.J. States, S. Swaminathan, and M. Karplus, *CHARMM: A program for macromolecular energy, minimization, and dynamics calculations*, J. Comput. Chem. 4 (1983), pp. 187–217.
[35] A. Smellie, S.L. Teig, and P. Towbin, *Poling: Promoting conformational variation*, J. Comput. Chem. 16 (1995), pp. 171–187.
[36] A. Smellie, S.D. Kahn, and S.L. Teig, *Analysis of conformational coverage. 1. Validation and estimation of coverage*, J. Chem. Inf. Comput. Sci. 35 (1995), pp. 285–294.
[37] A. Smellie, S.D. Kahn, and S.L. Teig, *Analysis of conformational coverage. 2. Applications of conformational models*, J. Chem. Inf. Comput. Sci. 35 (1995), pp. 295–304.
[38] C.A. Lipinski, F. Lombardo, B.W. Dominy, and P.J. Feeney, *Experimental and computational approaches to estimate solubility and permeability in drug discovery and development settings*, Adv. Drug Deliv. Rev. 23 (1997), pp. 3–25.
[39] C.A. Lipinski, F. Lombardo, B.W. Dominy, and P.J. Feeney, *Experimental and computational approaches to estimate solubility and permeability in drug discovery and development settings*, Adv. Drug Deliv. Rev. 46 (2001), pp. 3–26.
[40] S.E. O'Brien and M.J. de Groot, *Greater than the sum of its parts: Combining models for useful ADMET prediction*, J. Med. Chem. 48 (2005), pp. 1287–1291.
[41] A. Sali and T.L. Blundell, *Comparative protein modeling by satisfaction of spatial restraints*, Mol. Biol. 234 (1993), pp. 779–815.
[42] M.A. Martí-Renom, A.C. Stuart, A. Fiser, R. Sánchez, F. Melo, and A. Sali, *Comparative protein structure modeling of genes and genomes*, Annu. Rev. Biophys. Biomol. Struct. 29 (2000), pp. 291–325.
[43] S.F. Altschul, W. Gish, W. Miller, E.W. Myers, and D.J. Lipman, *Basic local alignment search tool*, Mol. Biol. 215 (1990), pp. 403–410.
[44] V.P. Jaakola, M.T. Griffith, M.A. Hanson, V. Cherezov, E.Y. Chien, J.R. Lane, A.P. Ijzerman, and R.C. Stevens, *The 2.6 Å crystal structure of a human A2A adenosine receptor bound to an antagonist*, Science 21 (2008), pp. 1211–1217.
[45] M.A. Hanson, V. Cherezov, C.B. Roth, M.T. Griffith, V.P. Jaakola, E.Y. Chien, J. Velasquez, P. Kuhn, and R.C. Stevens, *A specific cholesterol binding site is established by the 2.8 Å structure of the human β2-adrenergic receptor*, Structure 16 (2008), pp. 897–905.
[46] M.A. Laskowski, M.W. MacArthur, D.S. Moss, and J.M. Thornton, *PROCHECK: A program to check the stereochemical quality of protein structures*, J. Appl. Cryst. 26 (1993), pp. 283–291.
[47] A.L. Morris, M.W. MacArthur, E.G. Hutchinson, and J.M. Thornton, *Stereochemical quality of protein structure coordinates*, Proteins 12 (1992), pp. 345–364.
[48] R.W.W. Hooft, G. Vriend, C. Sander, and E.E. Abola, *Errors in protein structures*, Nature 381 (1996), pp. 272–272.
[49] M. Wiederstein and M.J. Sippl, *ProSA-web: Interactive web service for the recognition of errors in three-dimensional structures of proteins*, Nucl. Acids Res. 35 (2007), pp. W407–W410.
[50] M.J. Sippl, *Recognition of errors in three-dimensional structures of proteins*, Proteins 17 (1993), pp. 355–362.
[51] B. Gopalakrishnan, V. Aparna, J. Jeevan, M. Ravi, and G.R. Desiraju, *A virtual screening approach for thymidine monophosphate kinase inhibitors as antitubercular agents based on docking and pharmacophore models*, J. Chem. Inf. Model. 45 (2005), pp. 1101–1108.
[52] G. Jones, P. Willett, R.C. Glen, A.R. Leach, and R. Taylor, *Development and validation of a genetic algorithm for flexible docking*, J. Mol. Biol. 267 (1997), pp. 727–748.
[53] M.L. Verdonk, J.C. Cole, M.J. Hartshorn, C.W. Murray, and R.D. Taylor, *Improved protein–ligand docking using GOLD*, Proteins 52 (2003), pp. 609–623.
[54] A.M. Ter Laak, M.J. van Drooge, H. Timmerman, and G.M.D. den Kelder, *QSAR and molecular modelling studies on histamine H1-receptor antagonists*, Quant. Struct. Activ. Relation. 11 (2008), pp. 348–363.
[55] N. Bharatham, K. Bharatham, and K.W. Lee, *Pharmacophore identification and virtual screening for methionyl-tRNA synthetase inhibitors*, J. Mol. Graph. Model. 25 (2007), pp. 813–823.
[56] R. Kiss, Z. Kovari, and G.M. Keseru, *Homology modelling and binding site mapping of the human histamine H1 receptor*, Eur. J. Med. Chem. 39 (2004), pp. 959–967.
[57] C. Bissantz, P. Bernard, M. Hibert, and D. Rognan, *Protein-based virtual screening of chemical databases. II. Are homology models of G-protein coupled receptors suitable targets?* Proteins 50 (2003), pp. 5–25.
[58] F.F. Sherbiny, A.C. Schiedel, A. MaaB, and C.E. Muller, *Homology modelling of the human adenosine A2B receptor based on X-ray structures of bovine rhodopsin, the b2-adrenergic receptor and the human adenosine A2A receptor*, J. Comput. Aided Mol. Des. 23 (2009), pp. 807–828.
[59] K. Wieland, A.M. Ter Laak, M.J. Smit, R. Kuhne, H. Timmerman, and R. Leurs, *Mutational analysis of the antagonist-binding site of the histamine H1 receptor*, J. Biol. Chem. 274 (1999), pp. 29994–30000.
[60] A.B. Wagner, *SciFinder Scholar 2006: An empirical analysis of research topic query processing*, J. Chem. Inf. Model. 46 (2006), pp. 767–774.
[61] M. Haldeman, B. Vieira, F. Winer, and L.J.S. Knutsen, *Exploration tools for drug discovery and beyond: Applying SciFinder to interdisciplinary research*, Curr. Drug Discov. Technol. 2 (2005), pp. 69–74.